

PROSPECTS FOR POLARIZED ELECTRONS AT HIGH ENERGIES*

Charles Y. Prescott

Stanford Linear Accelerator Center

Stanford University, Stanford, California 94305

ABSTRACT

Neutral current and electroweak processes at high energies are well known to have large spin-dependent components. Proven techniques for producing polarized beams at storage rings and linear accelerators are now available. It is argued that use of polarized electrons in e^-e^+ annihilation at the Z^0 pole and above will provide the most precise tests of, and best experimental challenge to, the standard $SU(2) \times U(1)$ gauge theory model of electroweak interactions.

TABLE OF CONTENTS

- I. Introduction
- II. Comments on Electroweak Phenomenology
- III. Production of Polarized Beams in Storage Rings
- IV. Production of Polarized Beams for Linear Accelerators/Colliders
- V. Spin-dependent Effects in e^-e^+ Annihilation at the Z^0
- VI. Beyond the Z^0

*Work supported by Department of Energy, contract DE-AC03-76SF00515.

(Invited talk presented at the XVIII International School of Subnuclear Physics, Erice, Italy, July 31 - Aug. 11, 1980.)

I. INTRODUCTION

The past decade has witnessed a revolution in our understanding of particle interactions, rivaling the growth of quantum mechanics in the late 1920's. The emergence of gauge theories as the basis of weak, electromagnetic and strong forces will stand as a major milestone achieved during the 1970's. The decade of the 1980's promises to be the period of testing of these new fundamental ideas. The ability to make precise quantitative predictions within the framework of the gauge theories reinforces the interest in testing these new theories. In this special lecture I want to collect some of the ideas that I have had, and others have discussed, concerning the upcoming tests of $SU(2) \times U(1)$. In my view, these future tests will become precision tests of $SU(2) \times U(1)$, perhaps paralleling the traditional QED tests we have seen for quantum electrodynamic processes. It is my hope that future tests will lead us to the ultimate truth and provide the experimental support for electroweak theory at the level of confidence we now hold for QED processes. Polarized electron and positron beams should play a central role in the measurement of electroweak parameters. A strong preference for left-handedness in the weak part of the electroweak forces makes this possible. Unscrambling the details can best be done with the aid of polarized electron beams. Progress with polarization phenomena at storage rings and in linear accelerators brings experimental tasks within realization. This talk is a review of ideas on how polarized electrons may be used to test gauge theory models of electroweak interactions.

II. COMMENTS ON ELECTROWEAK PHENOMENOLOGY

The development of our present ideas of weak and electromagnetic forces can be traced a long ways back into history. Unification of electricity and magnetism occurred in the work of James Clerk Maxwell - 1868. This theory of electric and magnetic fields is today recognized as the original gauge theory. A new force

emerged from the discovery of radioactive nuclei. A form of the new "weak" force was first written down in 1934 by Fermi. He suggested a point-like four-vector lepton-hadron interaction lacking structure or dynamics. Yukawa introduced the idea of particle exchange as dynamical origin of forces. Forces can be characterized by their space-time transformation properties. Scalar, pseudo-scalar, vector, axial-vector or tensor forces, denoted by S, P, V, A, and T, respectively, form a complete set. The newly discovered weak forces were originally guessed to be S or P forces. In 1957, Feynman and Gell-Mann correctly suggested that the weak forces were of the V-A form, responsible for the large observed parity-violating effects seen in weak decays. Serious problems existed with the point-like form introduced by Fermi. Divergences existed which meant that the phenomenological description ultimately would fail at high energies. It was conjectured that the weak force would be mediated by a massive particle (the intermediate vector boson) which would damp the high energy behavior. Since beta decay processes occurred with charge transfer (both + and - signs occurring), the vector boson was assumed to come in two signs W^+ and W^- . It was natural to look for a neutral component of the weak force. An early suggestion that there would be a weak neutral current was published in 1957 by Zel'dovich. He suggested looking for weak-electromagnetic interference in polarized electron scattering and in optical rotation of the plane of linear polarization in heavy atoms. It was natural to try to incorporate the photon into a SU(2) triplet (W^+ , γ , W^-), as the basis for weak and electromagnetic forces. The possibility for such a structure being responsible for these forces was considered, most notably by Schwinger, Salam and others. Such a possibility suffers a number of difficulties. The possible interactions still contained some divergent pieces. The theory was not renormalizable. Masses of the particles were unequal. Perhaps most serious, the photon did not have the axial-vector piece of its interaction. Parity violation was absent, or

hidden, for the middle member of the triplet. Based on the evident failings of a simple triplet structure, more complicated structures were considered. Glashow, in 1960, discussed the idea of two massive neutral vector bosons occurring, with a fundamental mixing leading to a massless particle, the photon. In 1964, Salam and Ward introduced $SU(2) \times U(1)$ as a gauge group of the electroweak forces. Development of quantum field theory occurred rapidly during the early 1960's.

In 1967, Weinberg introduced a theory of leptons. It was the first comprehensive field theory which contained a mechanism for generating massive vector particles. The theory incorporated the concept of mixing introduced earlier by Glashow and the gauge group $SU(2) \times U(1)$. He introduced into the theory a scalar field which coupled to the leptons, leading to mass of the particles. Extra degrees of freedom, which in other theories led to predicted but unobserved massless particles, were successfully accommodated. The theory predicted existence of a new scalar particle or particles (the "Higgs" scalars) which remains today highly controversial, poorly understood, but fundamentally important because of the role played in the origin of mass. Weinberg assumed, but did not prove, that the theory was renormalizable. In 1971 't Hooft provided the rigorous proof that the Weinberg theory was indeed renormalizable. In 1971 Glashow, Iliopoulos, and Miani extended the Weinberg model to include couplings of quarks, and invented the charmed quark to explain the absence of strangeness changing neutral currents. These steps cleared up the many problems facing the unification of weak and electromagnetic forces and left open the prediction of neutral currents for leptonic and non-strange hadronic processes. In 1974, neutral currents were first observed in inelastic neutrino scattering in the Gargamelle bubble chamber at CERN. Parity violation in neutral currents was observed in 1978 in optical rotation of linearly polarized laser light in bismuth vapors at Novosibirsk and in inelastic scattering of polarized electrons from

hydrogen and deuterium at SLAC. From these various ideas we have a picture of what is now called THE STANDARD MODEL of weak and electromagnetic forces. Let me summarize some of the contents of this model.

(i) The forces are mediated by four vector bosons. In the unbroken form, there are four massless bosons, denoted (W^+, W^0, W^-) and B corresponding to the gauge group $SU(2) \times U(1)$. The triplet (W^+, W^0, W^-) couples to the "weak isospin" of the fermions, while the B couples to hypercharge, a combination of weak isospin and electric charge. Symmetry breaking and mixing lead to two physical particles:

$$\gamma = \sin\theta_w W^0 + \cos\theta_w B^0 \quad (1)$$

which is massless and arranged to have purely vector couplings. This particle is identified with the photon of electromagnetic interactions; and

$$Z^0 = \cos\theta_w W^0 - \sin\theta_w B^0 \quad (2)$$

a massive vector particle responsible for the neutral currents.

The Weinberg model contains the mass relations:

$$M_W = \frac{37.3 \text{ GeV}}{\sin\theta_w} ; M_{Z^0} = \frac{37.3 \text{ GeV}}{\sin\theta_w \cos\theta_w} ; M_\gamma = 0 . \quad (3)$$

(ii) All matter consists of fundamental constituents which are fermions. These are organized into three "generations", distinguished by masses which are light, intermediate, and heavy. It is presently assumed that there are three generations, but more may exist. These generations are:

$$\begin{pmatrix} u \\ d \\ e \\ \nu_e \end{pmatrix} \quad \begin{pmatrix} c \\ s \\ \mu \\ \nu_\mu \end{pmatrix} \quad \begin{pmatrix} t \\ b \\ \tau \\ \nu_\tau \end{pmatrix}$$

Of these fermions, only the t quark is yet unseen. The failure to observe $t\bar{t}$ states in e^+e^- annihilation at PETRA remains a puzzle, and possibly a problem for this picture. Tau neutrinos are indi-

rectly observed through missing momentum-energy balance in τ decays, are assumed to exist according to a normal sequential lepton pattern.

(iii) Weak electromagnetic currents are mediated by the four vector bosons. The charged currents, carried by W^\pm 's, couple to fermions by a V-A, or left-handed, form only. Hadronic transitions are $\Delta I = 1$ only. Neutral currents are a mixture of V and A, mostly of the V-A or left-handed type. In hadronic processes, both $\Delta I = 1$ and $\Delta I = 0$ terms are present. The photon, γ , couples by vector coupling only. The hadronic transitions are $\Delta I = 0$ or 1.

(iv) Neutral current couplings, as given in the standard model, depend on the weak isospin of the fermion involved. The standard model makes a choice of assignments:

$$\begin{pmatrix} \nu_e \\ e \end{pmatrix}_L, \begin{pmatrix} \nu_\mu \\ \mu \end{pmatrix}_L, \begin{pmatrix} \nu_\tau \\ \tau \end{pmatrix}_L, \begin{pmatrix} u \\ d \end{pmatrix}_L, \begin{pmatrix} c \\ s \end{pmatrix}_L, \begin{pmatrix} t \\ b \end{pmatrix}_L \quad \begin{array}{l} \text{left-handed} \\ \text{SU(2) doublets} \end{array}$$

and

$$e_R, \mu_R, \tau_R, \nu_e, \nu_\mu, \nu_\tau, u_R, d_R, c_R, s_R, t_R, b_R \quad \begin{array}{l} \text{right-handed} \\ \text{singlets.} \end{array}$$

Neutral currents couple according to the rule

$$g_{L(R)} = T_{3L(R)} - Q \sin^2 \theta_w \quad (4)$$

where $T_{3L(R)}$ is the third component of the weak isospin for the left (L) or right (R) component of the fermion, and Q is the electric charge. In the standard model $T_{3L} = +\frac{1}{2}$ for u, c, t quarks and for ν 's, and $-\frac{1}{2}$ for $d, s,$ and b quarks and for $e^-, \mu^-,$ and τ^- leptons. $T_{3R} = 0$ for all fermions. Often the sum and difference of g_L and g_R are used. They are denoted

$$g_V = \frac{1}{2}(g_R + g_L) \quad (5)$$

and

$$g_A = \frac{1}{2}(g_R - g_L)$$

Note that relation (4) predicts a different coupling for left- and right-handed components. Parity violation, a helicity dependence in scattering, is a direct result of equation (4) and the asymmetry between left- and right-handed components of fermions. This asym-

metry seems to be quite disturbing, and a number of authors prefer more complicated gauge theory structures which avoid this asymmetry. So far this asymmetry survives in all low energy tests of neutral currents.

Equation (4) also implies that neutral current couplings are the same for fermions which occupy similar positions in the three generations. For example, the e^- , μ^- , and τ^- leptons should have the same neutral current couplings. Similarly, the u, c, and t quarks should have the same couplings. Equation (4) is a statement of universality for the known generations. This prediction of universality of neutral current parameters at present is untested by any experiments. No neutral current parameters have been measured for second or third generation fermions.

(v) Neutral current processes are predicted to depend on a single parameter $\sin^2\theta_w$. This parameter is presently measured to have a value $.232 \pm .009$.¹ All experiments which are sensitive to $\sin^2\theta_w$ agree with this value. The standard model contains no prediction of the value of $\sin^2\theta_w$, although grand unification theories predict a value of $\sin^2\theta_w$ around .2.² The existence of a single parameter contains in it a prediction of universality of weak and electromagnetic couplings between components of different fermion generations. At present only e's and the light quarks u and d have their neutral current couplings measured. In the near future muon couplings should be measured, and later those of the τ lepton and heavy quarks.

(vi) The standard model predicts the existence of Higgs scalars (one or more) which couple to all fundamental fermions, but preferably to the heavy ones. This aspect of the standard model is still controversial, but very important. The Higgs scalars lead to generation of mass and may be the key to the mass spectrum of particles. At present there is no experimental evidence either supporting or contradicting this aspect of the standard model.

(vii) Parity violation is a central issue for neutral current

phenomena. The asymmetry between left- and right-handed couplings ($g_L \neq g_R$) leads to large spin-dependent effects in neutral current processes. Measurement of these spin-dependent terms may lead to the most precise experimental tests of the structure of neutral currents.

What then are the present issues? As experimental physics pushes energies up with new and larger accelerators, we will be addressing new problems. Is the standard model exact? Will $SU(2) \times U(1)$ survive precision tests like the more traditional QED tests of quantum electrodynamic processes? If not, in what ways does the standard model fail, and how may it be corrected? Universality is predicted, but experimentally untested. Neutral current couplings of e , μ , and τ should be equal. Universality of neutral current couplings should exist among quarks. New phenomena may emerge from production and decay of Z^0 's. Perhaps new generations of fermions will be seen or perhaps new particles will be seen which do not fit into the scheme. And finally the fundamentally important Higgs mechanism may be testable. Which possibility emerges as the important and new physics is difficult to foresee. Let me return to my main topic. Testing of neutral current phenomenology requires a careful study of the spin-dependent effects, and that can best be done with polarized electrons in the vicinity of the Z^0 pole. Why do I believe that? We now have ways to generate and select e_L and e_R easily. Measurement of neutral current parameters through weak-electromagnetic interference effects to obtain g_V and g_A for each of the lepton and quark species is possible with unpolarized beams, but at high energies counting rates will be low except at the Z^0 . Production of Z^0 's with polarized beams permits measurement of g_V and g_A parameters with good statistics. Finally, control of polarization permits control of spin-dependent effects in the Z^0 decay products, a fact important in the experimental technique. Let me now turn to a discussion of production of polarized electrons at high energies.

III. PRODUCTION OF POLARIZED BEAMS IN STORAGE RINGS

Production of polarized electrons has been the subject of extensive studies by many workers for a number of years. Interest among high energy physicists and accelerator physicists has grown strong in recent years, stimulated by storage ring physics, studies of nuclear structure, and electromagnetic and weak effects. I will review here briefly progress in polarized beam production from radiative beam polarization in storage rings.

Interest in expanding the physics information contained in e^+e^- annihilation has stimulated studies of polarization of e^+e^- beams in storage rings. In 1963, Sokolov and Ternov³ showed that transverse polarization for particles circulating in a uniform magnetic field would grow in time according to

$$P(t) = \frac{8\sqrt{3}}{15} [1 - \exp(-t/T_{\text{pol}})] \quad (6)$$

where the characteristic time is given by

$$\frac{1}{T_{\text{pol}}} = \frac{5\sqrt{3}}{8} \frac{e^2 h \gamma^5}{m^2 c^2 \rho^2} \quad (7)$$

where γ is the relativistic Lorentz factor, and ρ is the bending radius of the orbit. The result has been generalized by Baier and Katkov⁴ to include non-uniform fields and is discussed in review articles by Baier⁵ and Jackson.⁶

Spin motion in storage rings is not simple. In addition to the driving terms which lead to polarization described by equations (6) and (7), there are effects which work in the opposite direction, to depolarize a beam. Depolarizing effects come from spin resonances, stochastic processes and beam-beam interactions.⁷ Spin resonances occur when spin frequencies reach integral values relative to the orbit motion. The most prominent spin resonances are the integer resonances which occur every 440 MeV. Other resonances also occur. Stochastic depolarization arises from synchrotron radiation which can affect beam sizes and orbits. Beam-

beam effects likewise can influence beam dynamics, and the effect on beam polarization is not well understood or yet well measured. In the presence of depolarizing effects, the polarization given by equation (6) will reach a modified equilibrium value of

$$P_{\max} = \frac{8\sqrt{3}}{15} \frac{1}{1 + T_{\text{pol}}/T_{\text{depol}}}, \quad (8)$$

where T_{depol} is a characteristic time for depolarization.

Measurement of beam polarization and build-up times have confirmed the basic relations (6) and (7). Early work in the late 1960's led to measurements of beam polarization at Orsay at the storage ring ACO. Evidence for polarization was also reported from Novosibirsk and more recently from SPEAR.

Early measurements of polarization were made with a counter technique which measured internal ee scattering within the circulating bunch. This scattering is spin dependent, and the rate at which $\bar{e}\bar{e}$ pairs are counted outside the normal bunch profile was used to show existence of polarized beams. More recently, back-scattered laser beams have been used to probe circulating beams in storage rings. The spin-dependent terms in Compton scattering can be used to measure the beam polarization, and such measurements can be made rapidly. Figure 1 shows a SPEAR measurement using a

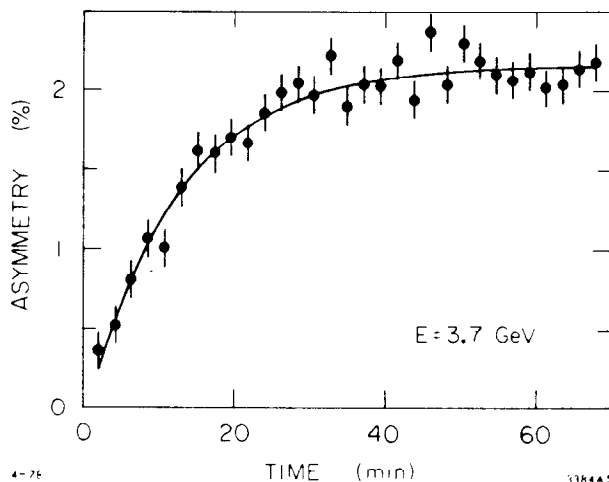


Fig. 1. An example of growth of beam polarization measured at SPEAR. The asymmetry refers to an up-down asymmetry in a detector looking at back-scattered laser photons which undergo Compton scattering off circulating SPEAR positrons.

polarized argon laser beam and a detector for backscattered photons capable of measuring an up-down asymmetry. The solid curve is a fit to the data with arbitrary normalization.

Beam codes exist which predict equilibrium polarization in the larger storage rings.⁸ Figure 2 is a calculation of maximum polar-

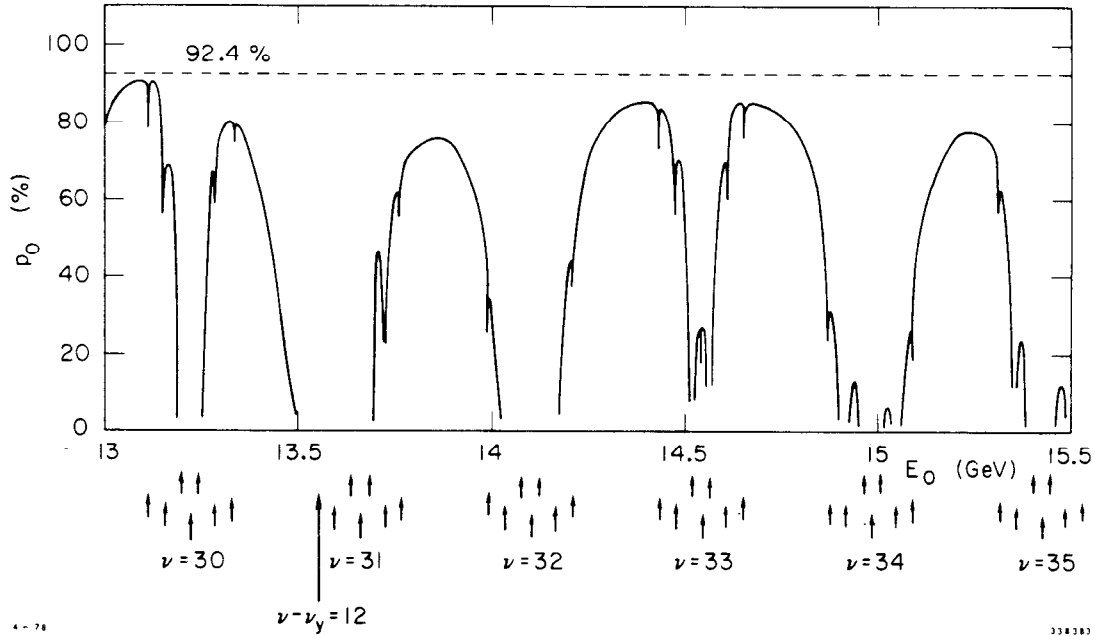


Fig. 2. A calculation of beam polarization at PEP (from Ref. 8). The arrows show positions of integer and sideband resonances. Conventional e^+e^- rings at high energies are expected to have complicated spin behavior.

ization versus beam energy for the PEP storage ring. The effect of closely spaced spin resonances becomes evident for the higher energy storage rings. At higher energies, the closely spaced spin depolarizing resonances may dominate over polarization effects, and at 100 GeV at LEP, Möhl and Montague⁹ argue that beams may not be polarized.

Storage rings naturally polarize beams transverse to the motion. The weak interactions are sensitive to longitudinal components of spin, so considerable interest in control of spin orientation exists. I will briefly mention two techniques. These techniques use the

precession of spin in magnetic fields to orient it properly. At high energies, the $g-2$ spin factor is such that spin precession is rapid relative to the precession of the momentum vector. Figure 3 shows a scheme of Schwitters and Richter¹⁰ in which the beam tra-

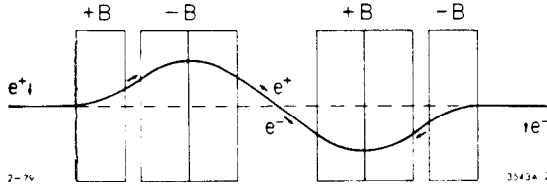


Fig. 3. The Schwitters-Richter scheme for producing longitudinal spins. The magnet arrangement is straightforward and relatively compact, but it introduces a tilted beam axis and severe problems with synchrotron radiation.

verses uniform, but alternating magnetic fields of a definite $\int B \, d\ell$. Spin precesses to a longitudinal orientation relative to the tilted beam direction. Both positrons and electrons should be polarized, with opposite spin projections, so at full polarization the cross section should vanish. This scheme has the unfortunate

disadvantage that weak and electromagnetic interactions are suppressed when the beams are fully polarized, and to study the weak interactions properly, one should separately control e^+ and e^- spins, or at least depolarize one of them.

A second scheme for controlling spin orientation in storage rings has been dubbed the "Siberian Snake" in honor of its inventors at Novosibirsk, Derbenev and Kondratenko.¹¹ In this scheme, magnets are placed in one section of the storage ring, arranged such that spin precesses 180° about the beam axis in passing through the "snake".

In principle, a single solenoid field could precess the spin about the axis. In practice, fields required are too large for conventional or superconducting solenoids. The snake scheme achieves the 180° spin rotation through the precession in a series of horizontal and vertical bends which restores the beam to its initial axis of motion. Figure 4 shows a sketch of the spin motion. At a point opposite the snake transverse components, both horizontal and vertical, after passing through the snake and re-

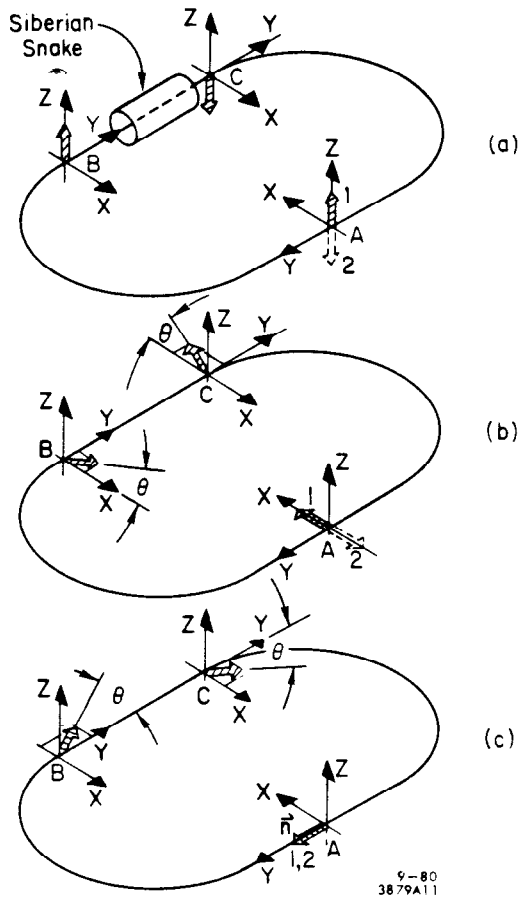


Fig. 4. Spin motion in a storage ring containing a "Siberian snake". Section BC contains a set of horizontal and vertical bends which approximates the spin motion of single uniform solenoidal fields. In Figs. 4(a) and (b), the transverse components return after a single pass with spin flipped. In Fig. 4(c) the longitudinal component is preserved at a point opposite the snake.

turning, have their signs reversed. That is, for transverse spin, no net polarization survives in such a machine. Longitudinal components are preserved after passing through the snake and returning.

The natural orientation for the spin is in the plane of the orbit and parallel to the beam at a point opposite the snake. Such ring configurations can be shown to have no problem with integer resonance depolarization. Normal radiative polarization does not occur, however, in such a modified ring. One must arrange to inject polarized electron and/or positrons into the ring. This leads me into the next topic, so let me conclude that future high energy storage rings may well provide polarized beams for e^+e^- annihilation, but such flexibility requires modifying in subtle ways the storage ring which already is a technically complicated device.

IV. PRODUCTION OF POLARIZED ELECTRONS FOR LINEAR ACCELERATORS/COLLIDERS

In quite recent times considerable interest and attention has been focussed on linear colliders as a new tool for e^+e^- collisions. A recent proposal at SLAC to accelerate e^- and e^+ bunches to 50 GeV, and bring them into collision, has been made. Linear accelerators are natural devices for accelerating polarized electrons. Longitudinal spin orientation is essentially undisturbed in the acceleration,¹² and estimates are that transverse components likewise suffer little depolarization.¹³

A program of polarized electron scattering has existed for some time at SLAC, and polarized electron beams have been accelerated routinely for a number of years. The first source of polarized electrons to be developed into an injector for the linac occurred in 1971. It was based on a Yale photoionization source using a UV flashlamp and a Li^6 atomic beam. More recently, development of a high intensity, laser driven, source began at SLAC in 1974.¹⁴ This latter technique offers the possibility of the future high current-high polarization polarized e^- beams needed for work in linear colliders.

Figure 5 is a sketch of a laser-driven solid state source similar to the one that operates at SLAC. Circularly polarized laser light falls on a gallium arsenide (GaAs) cathode, where internal electrons are pumped from the ground state levels into the crystal conduction band. Polarization of the electron population in the conduction band occurs when the laser beam is circularly polarized. For 100% circular polarization of the laser beam the internal polarization of the electrons is expected to be 50% in GaAs if we ignore depolarizing effects. Photoemission of conduction band electrons is possible when the GaAs crystal surface has cesium-oxygen monolayers deposited on it. This material lowers the potential barrier at the crystal-vacuum interface, and the photoemission currents are greatly enhanced. Proper activation of the

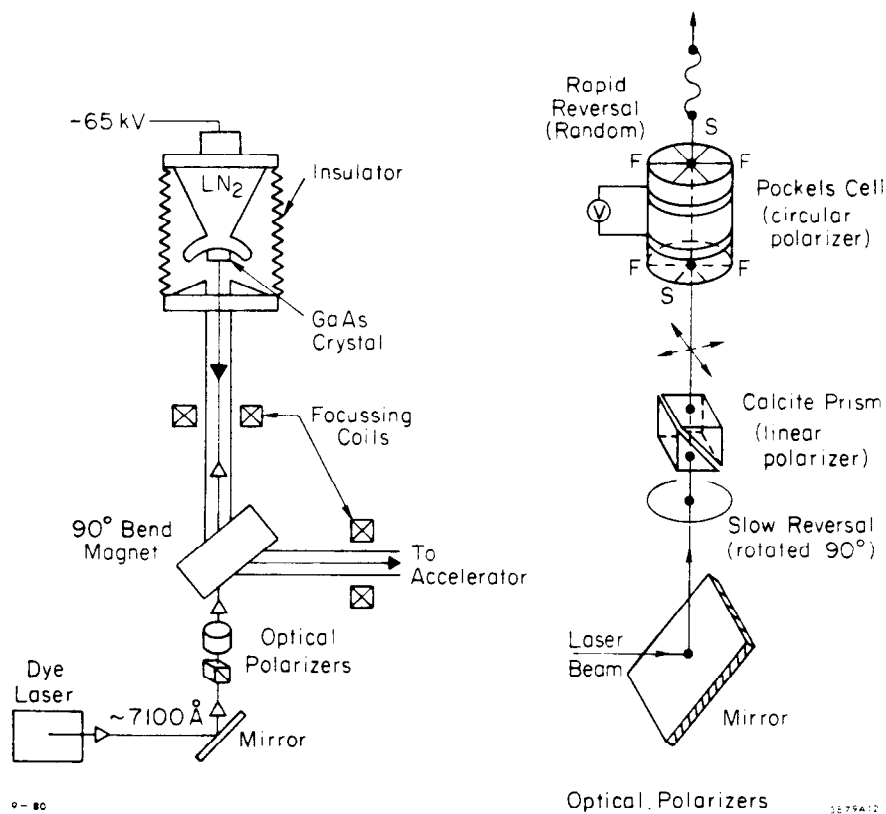


Fig. 5. A schematic of the SLAC GaAs polarized electron gun. A circularly polarized laser beam photoemits longitudinally polarized electrons from a GaAs crystal. An enlargement of the polarizing optics shows how polarization reversals may be achieved.

crystal surface requires some care, and to achieve long cathode lifetimes, exceptionally high vacuums are desirable in the region of the cathode. Therefore, considerable care must be taken in the design and construction of such a system.

High intensity beams have been achieved, up to 5×10^{11} electrons in 1.5 μsec pulses, and peak current densities of 180 Amps/cm^2 in short pulses. Polarization from GaAs crystals up to 40% are routinely obtained, and have been as high as 50% in tests. It is hoped that replacing the GaAs cathode with other semiconducting materials will substantially enhance the available polarization.¹⁵

Reversal of beam polarization is very easy in the GaAs source. The electron spin projection in the crystal is opposite that of the

laser photon. That is, positive circular polarization for a photon moving along the $+z$ axis gives electron spin pointing along $-z$. Since the electrons are photoemitted in the $-z$ direction, positive helicity results. If the photon circular polarization is reversed, electrons of negative helicity are photoemitted. Reversing the laser beam circular polarization flips the electron spin. In practice circular polarization can be quickly and cleanly reversed. Optical components exist which can reverse circular polarization with negligible influence on the laser beam direction or intensity. The ease of spin flips makes control of spin an important handle on control of systematics. In certain measurements, systematic errors can be virtually eliminated.¹⁶

V. SPIN-DEPENDENT EFFECTS IN e^-e^+ ANNIHILATION NEAR THE Z^0

I would now like to discuss some of the interesting spin related effects associated with e^+e^- annihilation near the Z^0 . Various aspects of these processes have been discussed in literature in different places, and I will try to give credit to those authors. My interest has been largely connected with the possibilities of polarized electron-unpolarized positron annihilation in linear colliders, so the discussion will be slanted in that direction. Many of the important effects occur in e^+e^- annihilation even for unpolarized beams, so some of these comments apply to LEP measurements as well. I will assume that one has a polarized electron beam, and that the helicity can be controlled. Curves will be marked according to e_L , 0, or e_R denoting left-handed, unpolarized, or right-handed electron beams. It is assumed that the positrons are unpolarized. For storage rings, positron polarization occurs naturally, but of the wrong sign to annihilate on electrons if precessed to the longitudinal orientation. Therefore, for these discussions to apply, storage rings would have to be arranged to depolarize selectively the positron beam. Techniques for doing this have been discussed.¹⁷ In practice polarized electron beams are not

completely polarized. Experimentally one must measure the beam polarization, but techniques for measuring electron beam polarization work well at high energies.¹²

(i) Total Cross Section Spin Dependence

The first and most important task for a new accelerator is to survey the lay of the land. Experimental measurements will probably begin with a scan over a reasonable range of energies. In the following discussions, the standard model of neutral currents is assumed, and for numerical estimates, the value $\sin^2\theta_w = .23$ is used.

Production of Z^0 's with polarized electrons on unpolarized positrons leads to polarized Z^0 's. The reason for this has to do with helicity conservation at the vertex. Polarized electrons pick out the proper spin state for positrons, from the unpolarized positron beam, to produce the spin 1 Z^0 boson polarized in the direction of the incident electron polarization (Fig. 6). The rate of pro-

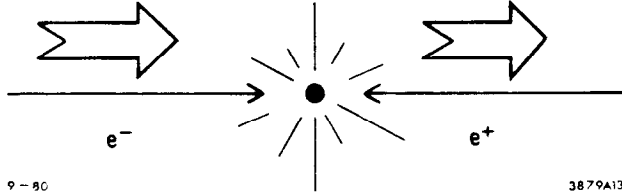


Fig. 6. Polarized electrons annihilate only on positrons of opposite helicity, giving spin 1 projection in the beam direction.

duction of Z^0 's could be enhanced if polarized e^+ beams were available, but experimentally unpolarized e^+ beams are much simpler.

The rate of production of Z^0 's is given by

$$\sigma(e^+e^- \rightarrow Z^0) \sim N^+ g_R^2 + N^- g_L^2 \quad (9)$$

where $N^+(N^-)$ is the number of $e_R(e_L)$ beam particles, given by

$$N^\pm = N_0 (1 \pm P_e) / 2 \quad (10)$$

where P_e is the beam polarization (for e_R , $P_e = +1$; for e_L , $P_e = -1$).

Using

$$g_R = \frac{1}{2}(g_V + g_A) \quad (11)$$

and

$$g_L = \frac{1}{2}(g_V - g_A)$$

then

$$\sigma(e^+e^- \rightarrow Z^0) \sim g_V^2 + g_A^2 + 2P_e g_V^e g_A^e \quad . \quad (12)$$

The Z^0 is expected to have a finite width, and a resonance shape.

A complete form for the cross section is given by¹⁸

$$\sigma(e^+e^- \rightarrow Z^0 \rightarrow f) = \left(g_V^e{}^2 + g_A^e{}^2 + 2P_e g_V^e g_A^e \right) \frac{2M_Z^3 \Gamma_f}{(s-M_Z^2)^2 + M_Z^2 \Gamma^2} \quad (13)$$

For electrons in the standard model

$$g_V^e = \frac{e}{\sin\theta_w \cos\theta_w} \{-1 + 4 \sin^2\theta_w\} ; \quad g_A^e = \frac{e}{\sin\theta_w \cos\theta_w} \quad . \quad (14)$$

Single photon exchange terms also contribute to $e^+e^- \rightarrow f$.

For completeness these terms must also be included, although at the Z^0 pole the single photon contribution is expected to be small, almost negligible. In Fig. 7, single photon exchange is included,

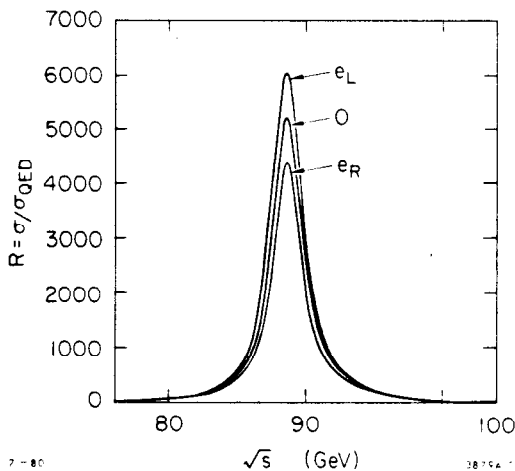


Fig. 7. The cross section ratio R at energies in the vicinity of the Z^0 pole, without radiative corrections. The standard model description for three generations and $\sin^2\theta_w = .23$ is used.

but radiative processes, which are significant, have been ignored. The effect of ordinary radiative effects are to lower and broaden the Z^0 peak, and to skew the distribution toward the higher energies.

Experimentally one measures an asymmetry defined as

$$A = \frac{\sigma_R - \sigma_L}{\sigma_R + \sigma_L} \quad (15)$$

where $\sigma_R(\sigma_L)$ is the cross section for $e_R(e_L)$ beams;

$$A = \frac{2g_V^e g_A^e}{g_V^e{}^2 + g_A^e{}^2} = -.16 \text{ for } \sin^2 \theta_w = .23 \quad (16)$$

This measurement could be made with considerable precision if polarized electrons are used at the Z^0 pole. It is a fundamentally important measurement, because the parameters g_V^e and g_A^e feed into all other measurements of spin-dependent effects at the Z^0 . In particular, accurate measurements of μ , τ and quark couplings will require electron parameters be measured precisely.

(ii) Polarization of the Z^0 's

Z^0 's will be produced with spin along the direction of the electron spin. The vector or axial-vector couplings pick out only one of the positron spin projections, and annihilation on the opposite spin does not occur. Polarized Z^0 's, however, are produced even with unpolarized beams, due to the unequal coupling strengths for e_L and e_R . One can easily estimate the Z^0 polarization for arbitrary electron polarization P_e . The number of positive helicity electrons is

$$N(e_R) = N_0 (1 + P_e)/2$$

and likewise for e_L ,

$$N(e_L) = N_0 (1 - P_e)/2$$

where N_0 represents the total number of electrons. The polarization of the Z^0 is

$$\langle P_{Z^0} \rangle = \frac{N_{Z^0}^+ - N_{Z^0}^-}{N_{Z^0}^+ + N_{Z^0}^-} = \frac{(1 + P_e)g_R^2 - (1 - P_e)g_L^2}{(1 + P_e)g_R^2 + (1 - P_e)g_L^2} .$$

Using equations (12), this becomes

$$\langle P_{Z^0} \rangle = \frac{2g_V^e g_A^e + P_e (g_V^{e^2} + g_A^{e^2})}{(g_V^{e^2} + g_A^{e^2}) + P_e (2g_V^e g_A^e)} \quad (17)$$

Figure 8 shows P_{Z^0} as a function of the electron polarization

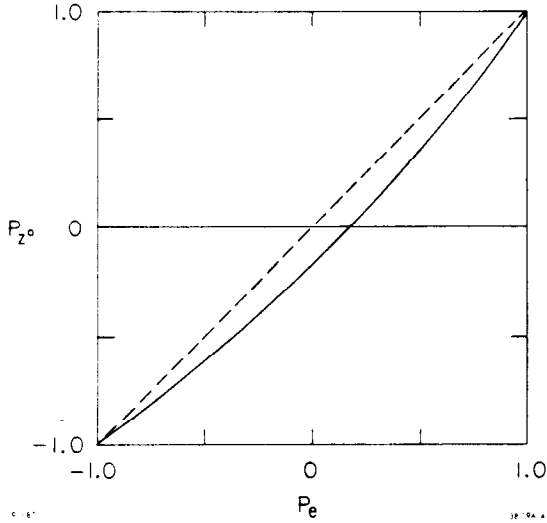


Fig. 8. The polarization of the Z^0 along the direction of the incident e^- beam, versus the beam polarization P_e . The solid curve is for $\sin^2 \theta_w = .23$, the dashed curve for $\sin^2 \theta_w = \frac{1}{4}$.

P_e . We observe that the Z^0 's are polarized even for unpolarized incident beams. This is to be expected because Z^0 's couple more readily to left-handed electrons than to right-handed electrons. For $P_e = 0$ and $\sin^2 \theta_w = .23$, the polarization of the Z^0 is $-.16$.

(iii) Charge Asymmetries in Final States

One example of final state effects arising from the Z^0 polarization is the charge asymmetry in $\mu^+ \mu^-$ final states. A charge asymmetry is defined as

$$A_{ch} = \frac{N(\mu^-) - N(\mu^+)}{N(\mu^-) + N(\mu^+)} \quad (18)$$

where the μ^- and μ^+ are detected in a well-defined solid angle. A simple estimate for A_{ch} can be obtained for forward ($\theta = 0$) production for a polarized Z^0 . Picture the Z^0 as aligned along the incident e^- direction. For a polarization P_Z , the number of Z^0 's

with ± 1 spin projection is

$$N_Z^\pm = N_Z(1 \pm P_Z)/2.$$

A Z^0 of $+1$ projection decays to a μ^- in the forward direction with a rate proportional to g_R^2 , and to a μ^+ in the forward direction with a rate proportional to g_L^2 . For -1 projections of the Z^0 , the g_R^2 and g_L^2 change places. The resulting charge asymmetry in the forward direction is

$$\begin{aligned} A_{\text{ch}} &= \frac{N(\mu^-) - N(\mu^+)}{N(\mu^-) + N(\mu^+)} \\ &= \frac{(1 + P_Z)g_R^2 + (1 - P_Z)g_L^2 - (1 + P_Z)g_L^2 - (1 - P_Z)g_R^2}{(1 + P_Z)g_R^2 + (1 - P_Z)g_L^2 + (1 + P_Z)g_L^2 + (1 - P_Z)g_R^2} \\ &= \frac{2P_Z(g_R^2 - g_L^2)}{2(g_R^2 + g_L^2)} \\ &= P_Z \frac{2g_V^\mu g_A^\mu}{(g_V^\mu + g_A^\mu)^2} \end{aligned} \quad (19)$$

Assuming $\sin^2\theta_w = .23$ and using the couplings of the standard model, the values of A_{ch} are $\mp .16$ for $P_e = \pm 1$, and $.026$ for $P_e = 0$. These values are for 0° μ -pair production. To calculate more realistic cases one must include single photon exchange terms and average over $\cos\theta$. Figure 9 shows the resulting charge asymmetry for μ -pairs, averaged over the forward hemisphere. The curves in Fig. 9 apply equally well to $\tau^+\tau^-$ final states, but not to e^+e^- final states where additional diagrams contribute to the scattering amplitude.

The polarization of the Z^0 is strongly enhanced by production with polarized beams, as shows in Fig. 8. The charge asymmetry should likewise be enhanced by polarized beams, and one expects measurements of neutral current parameters from charge asymmetries to benefit greatly from polarization. To illustrate the sensitivity

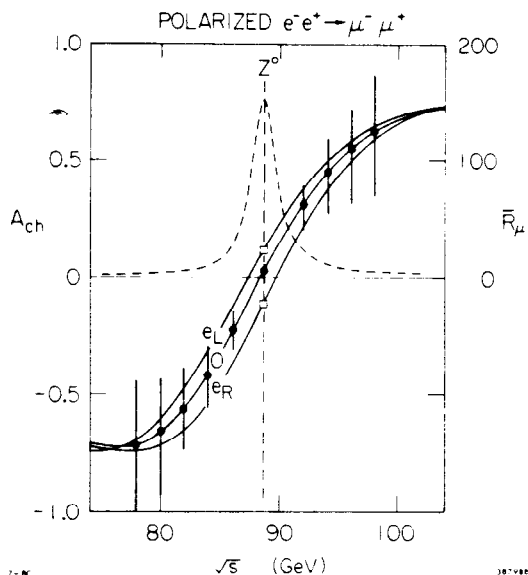


Fig. 9. The charge asymmetry for muon pairs versus center-of-mass energy for e_L , e_R and unpolarized beams. The points and associated errors compare two hypothetical experiments of 1,000 hours each, measuring muon neutral current parameters. Polarized beam measurements at the Z^0 pole (open squares) give substantially better accuracy than weak-electromagnetic interference measurements (solid dots) away from the peak of the Z^0 (see text).

to polarized electrons, a hypothetical 1,000 hour experiment at a luminosity of $10^{30} \text{ sec}^{-1} \text{ cm}^{-2}$ is shown in Fig. 9. One can measure charge asymmetries with unpolarized electrons at energies away from the Z^0 pole. Weak-electromagnetic interference leads to large asymmetries, but in regions where the cross section is small. If the 1,000 hour experiment is divided into ten 100 hour segments at ten different energies, the data and associated statistical errors that result are shown in Fig. 9. As a figure of merit on the sensitivity to charge asymmetries, the error on $\sin^2 \theta_w$ is calculated. The result is $\Delta \sin^2 \theta_w = .0027$. On the other hand, one could measure the same parameters using polarized electrons at the Z^0 pole where counting rates are high. The same 1,000 hours concentrating on the Z^0 pole, using a polarized electron beam (here assumed to be 50% polarized) yield $\Delta \sin^2 \theta_w = .0011$. Additional errors from systematic problems add to the statistical errors quoted here, but asymmetry measurements from use of polarized electron beams eliminate systematic errors from most sources. Although the calculation of $\Delta \sin^2 \theta_w$ may oversimplify the issues of sensitivity to gauge theory parameters, it does appear that measurements with polarized electrons offer significant improvement over other techniques for extracting gauge theory parameters.

Charge asymmetry effects also occur in the hadronic decays of the Z^0 . The basic couplings for $Z^0 \rightarrow q\bar{q}$ are specified by equation (4). One can calculate charge asymmetries for $Z^0 \rightarrow q\bar{q}$ final states. For example, Fig. 10 (a) shows results for $Z^0 \rightarrow u\bar{u}$ and Fig. 10 (b) for $Z^0 \rightarrow d\bar{d}$. The quarks will materialize as hadronic jets, and

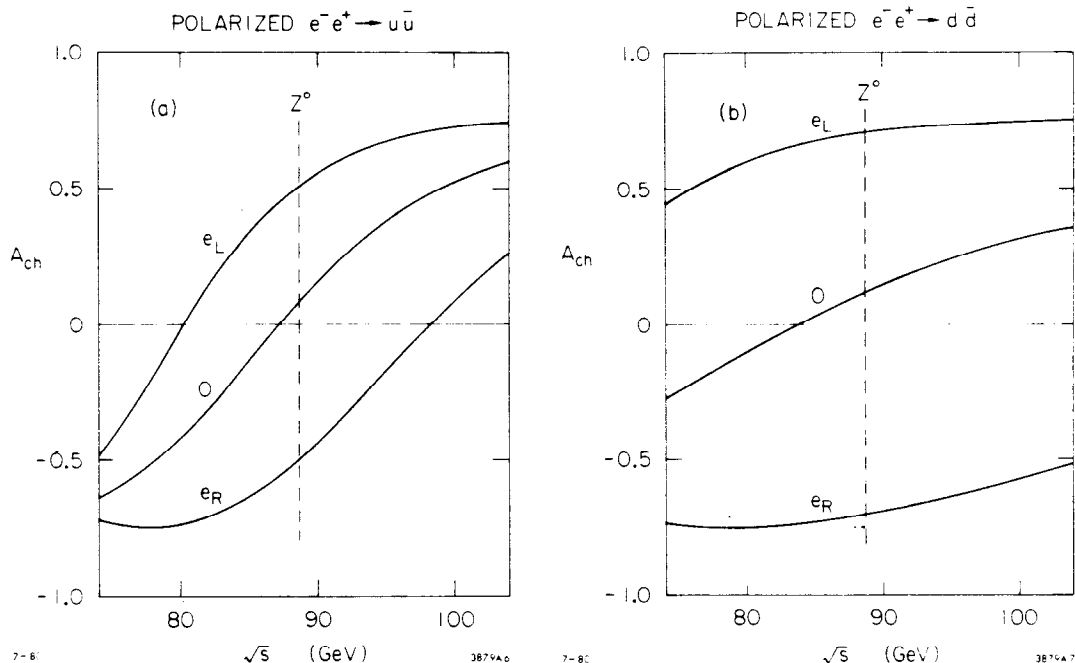


Fig. 10. Calculated charge asymmetries for $e^+e^- \rightarrow u\bar{u}$ jets and $e^+e^- \rightarrow d\bar{d}$ jets.

experimental identification of the quark flavor and charge from the hadronic debris may be difficult or impossible. Indeed, finding techniques for flavor discrimination will pose one of the most important and challenging experimental problems of high energies. Charge asymmetries are expected to be the same for $u\bar{u}$, $c\bar{c}$, and $t\bar{t}$ quark pairs, in the standard model at high energies, and likewise for $d\bar{d}$, $s\bar{s}$, and $b\bar{b}$ quarks. Universality of neutral current couplings is expected for fermions occupying similar slots in a generation, and tests of universality are very important. It may be more reasonable to expect experiments to combine jets together, averaging over flavor. This may avoid problems of flavor confusion

and may make tests more meaningful.

(iv) Final State Lepton Polarization

Final state leptons and quarks are expected to be polarized. It is simple to estimate the polarization of a final state fermion from $Z^0 \rightarrow f\bar{f}$, if one neglects the single photon contribution. For ± 1 (-1) projections of the Z^0 , as in Fig. 11, the rate of decay in the forward direction is proportional to g_R^2 (g_L^2). The polarization of the fermion f is

$$\begin{aligned} \langle P_f \rangle &= \frac{N_f^+ - N_f^-}{N_f^+ + N_f^-} = \frac{(1 + P_Z)g_R^2 - (1 - P_Z)g_L^2}{(1 + P_Z)g_R^2 + (1 - P_Z)g_L^2} \\ &= \frac{2g_V^f g_A^f + P_Z(g_V^{f^2} + g_A^{f^2})}{(g_V^{f^2} + g_A^{f^2}) + P_Z(2g_V^f g_A^f)} \quad \text{at } 0^\circ. \end{aligned} \quad (20)$$

For $e^-e^+ \rightarrow Z^0 \rightarrow \mu^-\mu^+$ (or $\tau^-\tau^+$) the polarization is $\langle P_{\mu,\tau} \rangle = \pm 1$ for $P_e = \pm 1$, and $-.31$ for $P_e = 0$, for $\sin^2\theta_w = .23$, in the forward direction.

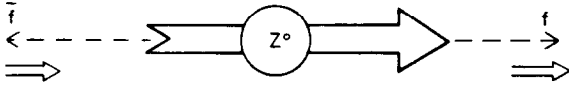
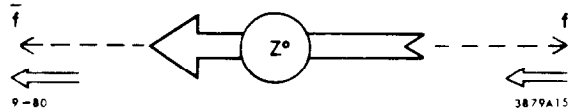


Fig. 11. Alignment of the Z^0 spin leads to final state fermion polarization.



For completeness one must include the one-photon exchange contribution, and average over solid angles.

Figure 12 shows the values for P_{μ^-} (or P_{τ^-}) averaging over the forward hemisphere, for a range of center-of-mass energies below and above the Z^0 .

The μ^- or τ^- polarization is a respectable -31% for unpolarized beams. This polarization occurs because the Z^0 prefers left-handed couplings and partially suppresses the right-handed compo-

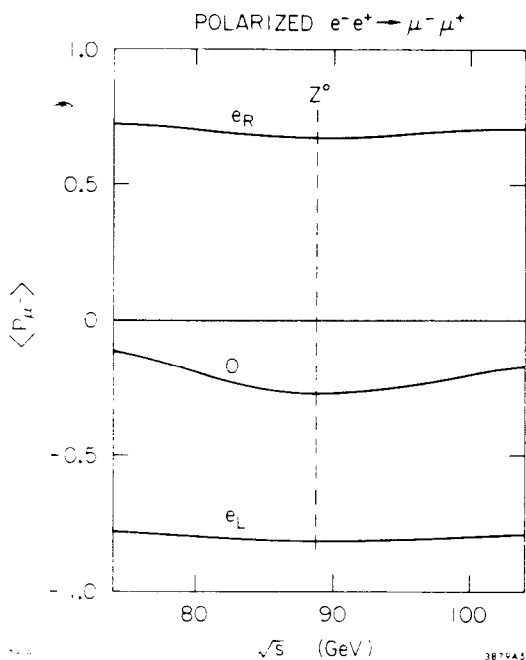


Fig. 12. Polarization of μ^- (or τ^-) versus center-of-mass energy, average over a 4π detector. These curves assume $\sin^2\theta_w = .23$.

nents. This large polarization will be very interesting in the case of τ 's produced off Z^0 's. Good measurements will result for the τ neutral current couplings. The decay is expected to be a good analyzer of τ spin.

(v) Two- and Three-Body Decays of the τ

The tau lepton has semi-leptonic and purely-leptonic decay modes. A two-body decay

$$\tau \rightarrow \pi\nu$$

has an expected 10% branching ratio, and should be an excellent analyzer of τ spin. Tsai¹⁹ has shown that this decay mode has an angular distribution

$$dN \sim (1 - h_{\pm} \cos\theta^*) d \cos\theta^* \quad (21)$$

in the center-of-mass of the τ , with helicity h_{\pm} , and in the lab

$$dN \sim 1 + \langle P_Z \rangle \frac{E_{\pi} - E_0/2}{E_0/2} \quad (22)$$

Figure 13 shows the predicted energy spectrum of the π , which is very sensitive to the incident beam polarization. Measurement of this decay mode should be clean, since identification of the τ is aided by the decay through other channels of its partner in the pair, the $\bar{\tau}$.

In a sample of 10^6 Z^0 's, approximately 6,000 $\tau \rightarrow \pi\nu$ events should be obtained. These should yield a good measurement of $\langle P_{\tau} \rangle$

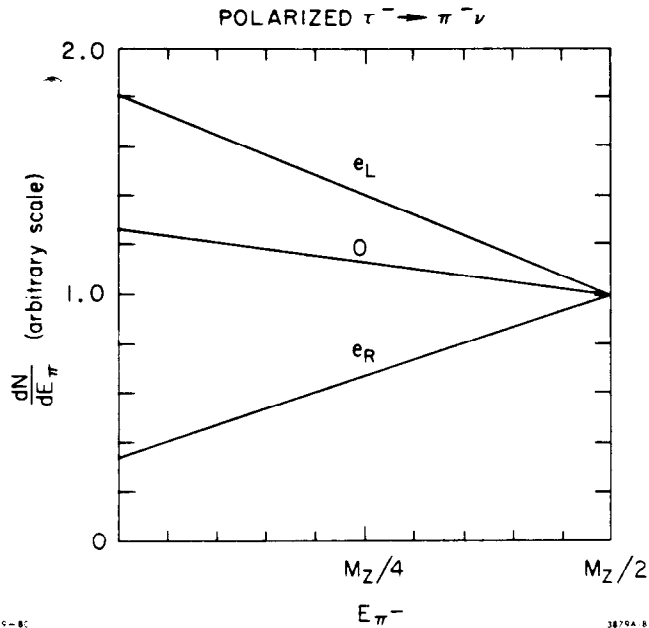


Fig. 13. The laboratory energy spectrum of pions for $\tau \rightarrow \pi\nu$ decays produced at the Z^0 pole, for e_L , e_R and unpolarized beams. Measurements of the pion spectrum should provide good values of the tau polarization and its neutral current couplings.

and through the relations similar to equation (20), a good value on its neutral current couplings g_V^τ and g_A^τ .

Two-body decays of the type $\tau \rightarrow \rho\nu$ are also expected to occur with a branching ratio of 23%.²⁰ These decays can be used to further improve measurements of the τ polarization.

Three-body decays of the tau (B.R. $\sim 16\%$ each)

$$\tau \rightarrow e \nu \bar{\nu}$$

and

$$\tau \rightarrow \mu \nu \bar{\nu}$$

likewise should teach us about tau spin and weak decays of the tau. Figure 14 shows the electron (or muon) energy spectrum assuming a standard V-A weak decay. The spectrum is significantly hardened for left-handed incident electrons. An average energy measurement should provide a sensitive parameter to compare to calculations. In a sample of 10^6 Z^0 's produced, approximately 20,000 decays should populate the distributions of Fig. 14, if standard model estimates remain valid. It is not unreasonable to expect 10^6 Z^0 's to be produced in a reasonable length of time.

Polarization effects also extend into the hadron jets. The primary quarks have large polarizations, but QCD effects which dress the quarks may also mask these large polarizations. At the present

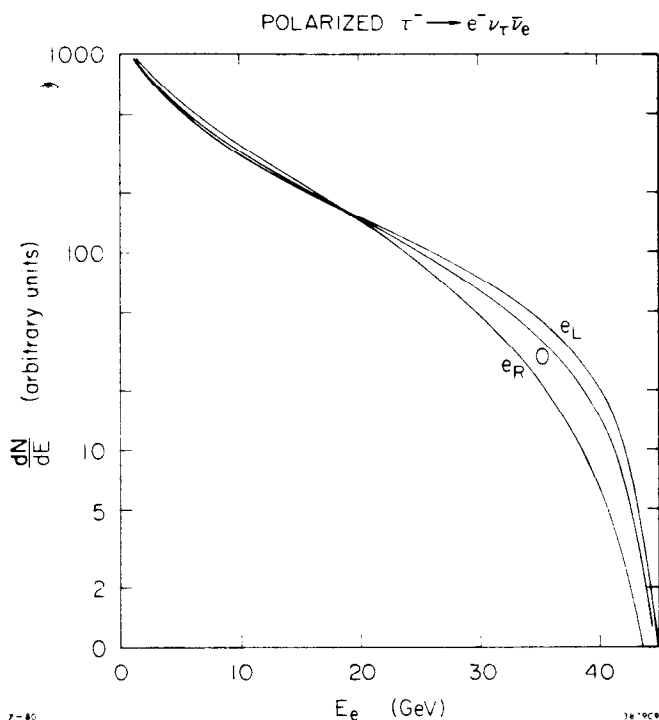


Fig. 14. The laboratory energy spectrum for electrons from $\tau^- \rightarrow e^- \nu_\tau \bar{\nu}_e$ produced at the Z^0 pole from incident electrons of e_L , e_R and 0 polarization. The mean electron energy is a good analyzer of tau polarization.

it appears unlikely that polarization effects in hadron jets will be useful. However, this may well be proven incorrect.

In summary, neutral currents are expected to

exhibit strong spin-dependent effects, and these effects are important to the experimental determination of neutral current parameters. Polarized beams greatly enhance these effects. From a careful study of these processes, precision tests of the standard model and neutral current parameters for the various quarks and leptons should emerge.

VI. BEYOND THE Z^0

I would like to conclude these remarks about prospects for polarized electron beams at high energies by looking beyond the Z^0 , to electroweak effects at even higher energies. It is clearly premature to worry at length or in too much detail when we still have much to learn yet at lower energies. Nevertheless, it is perhaps important to mention these other issues. The present proposal at SLAC to collide 50 GeV e^+ on 50 GeV e^- bunches in the single pass collider would not provide the capability to extend much beyond the presently expected value of the Z^0 mass. The CERN project LEP,

also in proposal stage now, does have the capabilities for higher energies. However, at these high energies beams at LEP may not be polarized. Nevertheless, I will conclude with a brief discussion of polarization phenomena which could provide important physics results.

(a) Single W Production

A process of considerable interest to physicists and importance to gauge theories, is the production of W's. Single W^- production can occur via the diagram shown in Fig. 15 (a). For $\sin^2 \theta_w = .23$, the mass of the W, and therefore the threshold for this reaction, is about 80 GeV. Cross sections for single W production will be very low near threshold, but are expected to grow somewhat at higher energies. Event rates of the order of 1 per day may be expected for luminosities of a few $10^{31} \text{ cm}^{-2} \text{ sec}^{-1}$.²¹ Although a lengthy run in a large detector may accumulate hundreds of these events, detection may not be easy because of backgrounds. The weak vertex of Fig. 15 (a) leads to a total vanishing of this

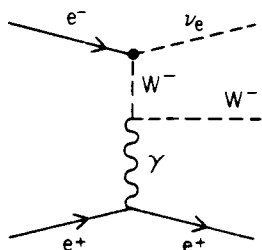
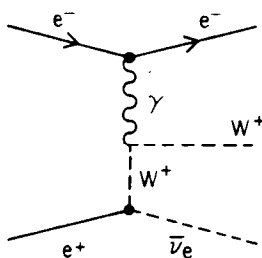


Fig. 15. Single W production diagrams for W^+ and W^- bosons. The weak charged current vertex for W^- production causes the cross section to vanish for e_R beams, but W^+ production should be insensitive to e^- beam polarization.



9-80

3879A16

process for e_R polarizations. This fact may have considerable practical consequence, allowing for subtraction of uninteresting background signals. The production of W^- 's, through the diagram in Fig. 15 (a), and the production of W^+ 's through the process shown in Fig. 15 (b), should show quite different spin dependence. The W^- signal will have a large asymmetry between e_R^- and e_L^- , but the W^+ signal at the same time should show almost no

asymmetry. Detection of single W^+ and W^- events may be experimentally quite difficult, since the W 's will fragment into hadron jets. The spin-dependent structure described above could be an important tool in the experimental bag of tricks used to find the W 's.

(b) Testing of Gauge Theory Models Beyond $SU(2) \times U(1)$

Considerable interest in left-right symmetric models remains although low energy neutral current experiments argue against some of the early ones. In models containing two Z^0 's accommodating the low energy neutral current data requires a lighter Z^0 of mass close to that predicted by the standard model, and a heavier one with mass > 200 GeV. The lighter Z mass differs from that predicted by the standard model, but can be close enough that it may be difficult to know if the standard model, including radiative corrections and QCD corrections, is in difficulty. A more sensitive test of two Z models comes from charge asymmetry measurements above the first Z^0 . In this region charge asymmetry measurements are sensitive to interferences, and the presence of a Z_2^0 would likely be seen here first. As discussed earlier, polarized e^- beams can provide a very practical experimental aid in eliminating many systematic uncertainties in these measurements.

(c) $e^+e^- \rightarrow W^+W^-$

Diagrams which contribute to this process are given in Fig. 16. The polarization dependence has been studied in detail for both incident and final polarization states, in general form and in the standard model.²² Gaemers and Gounaris emphasize that the important thing is to extract from this process the trilinear boson couplings for the γWW and ZWW vertices. They point out that in any gauge theory these interactions should obey C, P, and T invariance and the W should have definite values for magnetic dipole and electric quadrupole moments for couplings to the γ and

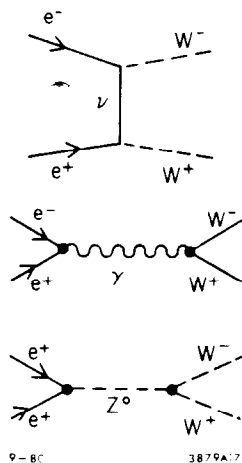


Fig. 16. W-pair production diagrams.

Z boson. The W-pair production provides the opportunity to measure these couplings. Cross section estimates coupled to reasonable luminosity estimates at LEP indicate a few thousand events could result from a few months of high energy running. However, most of the contribution comes from the "boring" ν exchange diagram. This term involves no controversial aspect of weak-electromagnetic interactions. Observing the small "interesting" part may not be possible. Measurement of asymmetries between e_L and e_R should be compared with these predictions. Any significant deviation could be evidence for problems with the three vector boson vertex.

At higher energies, the process $e^+e^- \rightarrow ZZ$ could likewise expose problems with specific gauge theories. This process is also discussed in Ref. 22, and if the energy is available may ultimately provide interesting data.

Let me conclude. The standard model of weak and electromagnetic processes predicts a strong dependence on the polarization of incident beams. This polarization dependence can be studied using polarized electrons annihilating on unpolarized positrons. It is not necessary to polarize the positron beam, although it is natural for this to occur in storage rings. For linear colliders, a single polarized electron beam is ideal and practical. Control of spin of electron beams has been shown to be practical in linear accelerators, and rapid reversals of spin can eliminate many sources of systematic errors. Through use of polarized beams, many neutral current parameters can be measured at the peak of the Z^0 pole, with the practical advantage of providing higher counting rates than obtained away from the Z^0 pole where γ - Z interference occurs. Polarization effects propagate through the Z^0 into the final state. Charge asymmetries and final state polarization are

important effects sensitive to incident polarization. Precision tests of gauge theory predictions should result from polarized beam measurements. Beyond the Z^0 pole lies the region of single W, W-pair, and Z^0 -pair production providing additional tests of electroweak models.

I wish to acknowledge contributions from several colleagues at SLAC. Charlie Sinclair, who has played a central role in bringing the laser-driven GaAs source into operation, continues the work for higher polarization. Through his efforts prospects for suitable polarized beams for colliders seem bright. Tom Tsao and Fred Gilman were very kind to help with some of the calculations, and provided many useful comments.

REFERENCES

1. P. Langacker et al., Proceedings of Neutrino 79, Bergen, Norway, June, 1979.
2. A.J. Buras et al., Nucl. Phys. B135:66 (1978).
3. A.A. Sokolov and J.M. Ternov, Sov. Phys. Dokl. 8:1203 (1964).
4. V.N. Baier and V.M. Katkov, Phys. Lett. 24A:327 (1967); and Sov. Phys. JETP 25:944 (1967).
5. V.N. Baier, Sov. Phys. Usp. 14:695 (1972).
6. J.D. Jackson, Rev. Mod. Phys. 48:417 (1976).
7. R.F. Schwitters, Conference Proceedings on High Energy Physics with Polarized Beams and Targets, Argonne (1978).
8. A.W. Chao, SLAC Technical Note PEP-263 (1978).
9. D. Möhl and B.W. Montague, Nucl. Instrum. Methods 137:423 (1976).
10. R. Schwitters and B. Richter, SLAC Technical Note PEP-87/SPEAR 175 (1974).
11. Ya.S. Derbenev and A.M. Kondratenko, Novosibirsk Preprint 76-84 (1976).
12. P.S. Cooper et al., Phys. Rev. Lett. 34:1589 (1975).
13. R.H. Helm and W.P. Lysenko, SLAC-TN-72-1 (1972).

14. E.L. Garwin et al., Helv. Phys. Acta 47:393 (1974); and SLAC-PUB-1576 (1975).
15. C.K. Sinclair, Stanford Linear Accelerator Center, Stanford, California, private communications.
16. These techniques were used in measuring parity violation due to weak-electromagnetic interference in inelastic electron scattering, C.Y. Prescott et al., Phys. Lett. 77B:347 (1978).
17. W. Toner, 1974 PEP Summer Study Proceedings PEP-137 (1974).
18. J. Ellis and M.K. Gaillard, CERN REPORT 76-18 (1976).
19. Y.S. Tsai, Phys. Rev. D4:2821 (1971).
20. Y.S. Tsai, SLAC-PUB-2105 (1978).
21. M. Davier, Proceedings of the LEP Summer Study, Les Houches and CERN, 1978, CERN 79-01 (1979).
22. K.J.F. Gaemers and G.J. Gounaris, Z. Physik C, Particles and Fields I:259 (1979).